

Stable spiral structures and their interaction in two-dimensional excitable media

Roman M. Zariiski*

*Department of Computer Science, Montclair State University, Upper Montclair, New Jersey 07043*Arkady M. Pertsov[†]*Department of Pharmacology, SUNY Upstate Medical University, Syracuse, New York 13210*

(Received 2 August 2002; published 16 December 2002)

We study properties and interactions of stable spiral structures in two-dimensional excitable media modeled by equations of FitzHugh-Nagumo type. The presented results rely on the media ability to support unexcited spiral cores. Comparative frequency and dynamics analysis is done for a single spiral, an oppositely charged bound pair, and multiarmed spirals. Higher-frequency structures can attract, repel, or break up structures with lower frequencies. All pairwise reactions are described. A three-armed spiral and a two-armed spiral of opposite charge can form a stable “molecule.” A system with high initial vortex concentration evolves according to the described reactions and exhibits three levels of self-organization. In our simulations such evolution led to formation and domination of persistent three-armed spirals.

DOI: 10.1103/PhysRevE.66.066120

PACS number(s): 82.40.Ck, 05.65.+b, 89.75.Kd

I. INTRODUCTION

Spiral waves have been observed and studied in a variety of physical, chemical, and biological systems. Many of these systems can be classified as excitable media, which are known to support persistent rotating vortices of excitation that emit waves of spiral shape. Examples include waves of chemical activity in Belousov-Zhabotinsky (BZ) reaction [1], electrical activity in cardiac tissue [2], aggregation of starving slime mold amoebae (*Dictyostelium discoideum*) [3], and catalytic reactions on platinum surface [4]. Spiral waves in excitable media are a remarkable example of self-organization in the underlying physical systems and have been studied extensively. An important question for understanding complex dynamics in excitable systems is interaction of vortices with each other. Interacting spiral waves may play a significant role in the development of ventricular fibrillation, the most dangerous type of a cardiac arrhythmia [5]. However, relatively little is known about interaction of many spiral waves, some important questions are still open, and the “big picture” is unclear.

A series of studies [6–13] have addressed interaction of several spirals in two-dimensional excitable media, both experimentally and numerically. Among reported multispiral structures are a symmetric bound pair of two vortices of opposite topological charge (chirality) [8,13] and ensembles with two or more vortices of the same chirality [6,8,9,12], which we will refer to as multiarmed spirals. An oppositely charged bound pair, or dipole, is characterized by a drift along its symmetry axis [8,13], and in some cases can undergo a symmetry-breaking instability and disintegrate [10,11]. Vasiev, Siegert, and Weijer [12] have shown that stable multiarmed spirals can arise spontaneously from sev-

eral like-charge single spirals if their tips are less than one wavelength apart.

Stable bound vortex pairs of opposite charge have also been reported among solutions of the complex Ginzburg-Landau equation [14,15], which governs weakly nonlinear oscillatory media, e.g., in nonlinear optics. Multiarmed spirals have been observed in Rayleigh-Bénard convection [16], a system which is not an excitable medium. The focus of this paper, however, is on excitable media.

Questions about spiral interaction that are still open include systematic classification of stable spiral structures, description of their pairwise interactions, and evolution of a system with a high concentration of excitation vortices. To answer these questions, we model a generic excitable medium with simple differential equations of FitzHugh-Nagumo (FHN) [17] type that support spiral waves with a stationary core, i.e., when the trajectory of the tip of an isolated spiral wave is a circle. The details of the model are given in Sec. II.

Spiral cores are typical in BZ reactions, reentrant cardiac excitation waves, and *Dictyostelium discoideum* aggregation. Moreover, cores are responsible for what we believe is the primary vortex interaction mechanism [7,18,19]. According to this mechanism, when a wave front collides with a vortex at or near its tip, the core of that vortex shifts to a new position. This mechanism works both at short distance, e.g., between vortices within an ensemble, and at long distance, when vortices or groups of vortices are arbitrarily far from each other. Thus, cores are essential for the phenomena of structure formation and spiral drift in the presence of other spirals. The size of a core is primarily determined by the medium excitability. If excitability is very high, there might be no core at all. In this study, we model media with core diameters that are comparable with the wave width (from front to tail) and that are about 10–20% of isolated spiral wavelength (from front to front), which is consistent with physical examples.

Figure 1 shows two different types of like-charge spiral ensembles that have been called “multiarmed spirals” in lit-

*Corresponding author. Email address: zariiski@roman.montclair.edu; URL: <http://roman.montclair.edu>

[†]Email address: perzova@upstate.edu; URL: <http://web.upstate.edu/PERZOVA/>

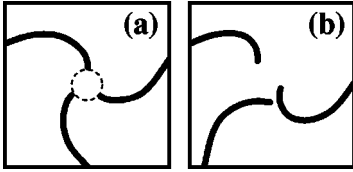


FIG. 1. Schematic drawing of two types of like-charge spiral ensembles. (a) Noncolliding vortices with a shared core (dashed circle). (b) Intermittently colliding vortices (M_n). Excited and unexcited areas are shown in black and white, respectively.

erature. The first type is defined by the lack of collisions between waves, which happens when vortex tips rotate about the same core [Fig. 1(a)] or in some cases of overlapping cores. The second type [Fig. 1(b)] is characterized by a complex dynamics that involves intermittent pairwise collisions of vortices at or near their tips.

In this investigation we focus on *stable* structures, i.e., structures that tend to restore and maintain their form and behavior in the presence of perturbations and disturbances. A single isolated vortex and a bound dipole are examples of such stable structures. We will refer to them as S and D , respectively. Only the second type of multiarmed spiral [Fig. 1(b)] exhibits such stability in our model. Moreover, this is the only type that formed spontaneously in our simulations from several like-charge S spirals. We will refer to an n -armed spiral of this type as M_n and will use a positive or negative sign to specify, respectively, the clockwise or counterclockwise direction of rotation. For example, Fig. 1(b) shows M_3^+ . The dynamics of M_2 was described by Ermakova, Pertsov, and Shnol [8] as a precession of two separate cores around each other. A multiarmed spiral M_3 lacks rotational symmetry and has a more complex dynamics.

Numerical simulations revealed that multiarmed spirals M_n are stable for low values of n and break up if n is high. In Sec. III, we present frequency analysis for stable S , D , and M structures, describe pairwise reactions between them, and trace the evolution of a system with high initial vortex concentration. The significance of the results is discussed in Sec. IV.

II. MODEL AND METHODS

We adopted the same model as was used by Ermakova, Pertsov, and Shnol [8]. The equations are

$$\frac{\partial u}{\partial t} = \Delta u + f(u) - v, \quad (1)$$

$$\frac{\partial v}{\partial t} = \frac{u - v}{\tau(u)}, \quad (2)$$

where $u = u(x, y, t)$ is the excitation function and $v = v(x, y, t)$ characterizes the recovery process. Piecewise-linear function $f(u)$ and piecewise-constant function $\tau(u)$ are given by

$$f(u) = -C_1 u \quad \text{if } u < E_1$$

$$f(u) = C_2(u - a) \quad \text{if } E_1 \leq u \leq E_2$$

$$f(u) = -C_3(u - 1) \quad \text{if } u > E_2, \quad (3)$$

$$\tau(u) = \tau_1 \quad \text{if } u < B_1$$

$$\tau(u) = \tau_2 \quad \text{if } B_1 \leq u \leq B_2$$

$$\tau(u) = \tau_3 \quad \text{if } u > B_2, \quad (4)$$

where $C_1 = 4$, $C_2 = 0.75$, $C_3 = 15$, $E_1 = 0.018$, $\tau_1 = \tau_3 = 0.5$, $\tau_2 = 16.66$, $B_1 = 0.01$, $B_2 = 0.95$, $a = E_1(C_1 + C_2)/C_2$, and $E_2 = [(C_1 + C_2)E_1 + C_3]/(C_3 + C_2)$.

This is a strongly nonlinear reaction-diffusion system that models behavior of a generic two-dimensional excitable medium. We solved this system numerically on rectangles of various sizes with Neumann (no-flux) boundary conditions. An explicit difference scheme was constructed based on Euler integration. Computations for that scheme were carried out on a parallel cluster using a simple ‘‘domain slicing’’ algorithm [20]. In most experiments, we used a spatial step $\Delta x = 0.6$ distance units (d.u.) and a time step $\Delta t = 0.05$ time units (t.u.). For some simulations of long-term evolution on a large medium we also used $\Delta x = 1.2$ and $\Delta t = 0.1$. To verify that the scheme is well behaved, we used $\Delta x = 0.3$ and $\Delta t = 0.02$. Depending on the type of simulation the size of rectangular grid varied from 200×200 to 3000×3000 nodes.

The only parameter in Eqs. (3) and (4) that we varied in some experiments was C_2 , which determines the medium excitability and, consequently, the size of spiral cores. Unless otherwise noted, C_2 is 0.75, the base value used in most simulations. It corresponds to the core diameter of approximately ten spatial units or 15% of the wavelength of S . Higher values of C_2 correspond to higher excitability and smaller spiral cores.

Initial conditions for the simulations were produced by using two kinds of rectangular ‘‘patches’’ as shown in Fig. 2. A square patch [Fig. 2(a)] was used to generate a bound dipole D . ‘‘Spiral gas’’ with high vortex concentration was created by a superposition of a large number of square patches placed at random locations with random angle and magnitude of the shift between the u and v components.

A combination of ‘‘stripe’’ patches [Fig. 2(b)] was used to initiate multiarmed spirals. Figure 2(c) shows how M_3 can be generated. This approach also works for M_2 and M_4 . Figure 2(d) shows an initial stripe configuration that develops into a four-armed spiral. Depending on the exact stripe positions, both M_4 and a four-armed spiral with a common core can be initiated.

Spiral tips were detected as points where $u \approx 0.2$, while $\partial u / \partial t \approx 0$. The direction of the cross product $\nabla u \times \nabla v$ at those points determines the vortex chirality.

III. RESULTS

A. Stable structures

Numerical simulations for the base core size, i.e., with $C_2 = 0.75$, demonstrated stability of M_2 and M_3 . These structures are formed whenever two or three like-charge vor-

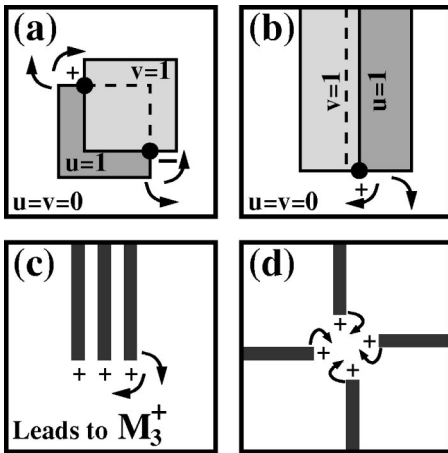


FIG. 2. Generating initial conditions with rectangular patches. (a) A square patch. Dark and light shades correspond to excited and refractory medium, respectively. If the tip formation points (shown as black circles) are kept approximately two spiral cores apart, this patch develops into a D . (b) A stripe patch. (c) Three parallel stripe patches that are less than one S wavelength apart develop into M_3 . (d) Initiating a four-armed spiral with four stripe patches.

tices come closer to each other than approximately one wavelength of S . After that, the vortices exhibit strong binding to each other and can withstand significant external disturbances. The binding occurs due to an appropriate adjustment of core positions during repeated arm collisions.

It is easy to initiate M_4 using initial conditions similar to the configuration shown in Fig. 2(d), with the four tip formation points within one wavelength of S from each other. However, as Fig. 3 demonstrates, this structure is unstable. Generally, multiarmed vortices other than M_2 and M_3 were rarely observed in our simulations. They appear transiently and eventually transform into either M_2 or M_3 .

Thus, the only stable spiral structures are S^\pm , D , M_2^\pm , and M_3^\pm . Frequency calibration was carried out for these structures by placing a simulated probe at a distance from their centers and recording the times between consecutive wave fronts. The results of these measurements are shown in Fig. 4. The distance between waves emitted by M_2 varies periodically. Variations for M_3 have a more complicated pattern, reflecting the complex dynamics of vortex tips within this structure. Triplet M_3 is the fastest stable source, with an

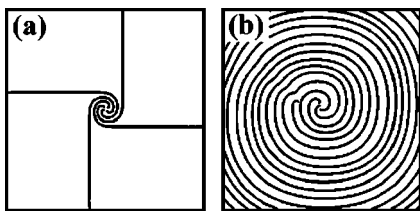


FIG. 3. A simulation result demonstrating instability of M_4 . (a) An M_4 structure can be initiated with four stripe patches in a cross-like configuration. (b) If the initial configuration has some asymmetry or if perturbations are present, the M_4 quartet eventually expels one vortex and reduces to a stable M_3 triplet. This can be summarized symbolically as $M_4^+ = M_3^+ + S^+$.

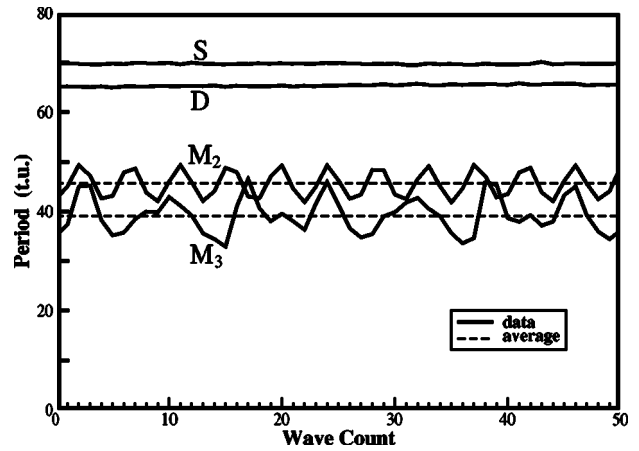


FIG. 4. Periods of waves emitted by stable spiral structures as sensed by a distant probe for 51 consecutive wave fronts. Measurements for D can vary slightly due to Doppler effect. The average frequencies sent to the medium by D , M_2 , and M_3 are, respectively, 7%, 52%, and 78% higher than the frequency of S .

average frequency 1.78 times higher than the frequency of S , the lowest stable structure. This confirms that M_3 is very different from a three-armed spiral with a common core, which, assuming no interaction between its arms, should have a frequency three times higher than the frequency of S .

Similar results hold in some neighborhood about $C_2 = 0.75$, including 0.78, which corresponds to twice smaller cores. For higher values of excitability C_2 , such as 0.85, cores become negligibly small compared to the wave dimensions, which impairs the principal spiral interaction mechanism that we consider in this study. At $C_2 = 0.72$, which corresponds to cores that are approximately two times larger than at the base value, M_3 becomes less stable and easily reduces to M_2 by expelling one S . Lower values of excitability quickly lead to very large cores, violating our assumptions. For such cores, e.g., at $C_2 = 0.68$, we were able to initiate a four-armed spiral with noncolliding arms that emits a frequency four times higher than a single spiral.

B. Reactions

1. Overview

When two excitation waves collide, they annihilate. As shown in Fig. 5, if the frequency of one of two spiral structures is higher, the interface where their waves meet moves in the direction of the slower source. More interesting is the second stage of interaction, when the waves of the stronger

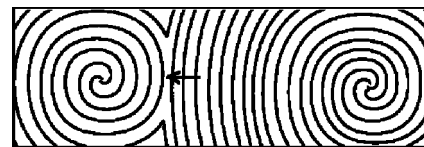


FIG. 5. First stage of interaction between two spiral structures occurs along the interface of their wave patterns. The source on the right (M_3^+) has a higher frequency. Hence, the interface is moving towards the “weaker” source (M_2^+) as shown with an arrow.

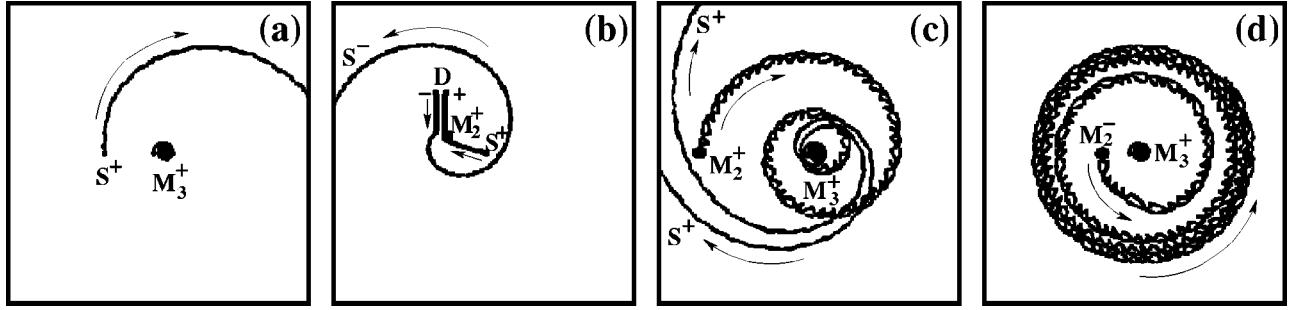


FIG. 6. Examples of reactions between stable “particles.” Spiral tip trajectories are shown as black curves and circles. (a) M_3 repels S . (b) S is attracted to a drifting D ; their collision leads to formation of a stable M_2 , with one S expelled. (c) M_3 attracts M_2 of the same sign; after their collision a transient M_5 structure expels two S particles and reduces to the original M_3 . (d) Depending on the distance, M_3 either repels or attracts M_2 of the opposite sign; in both cases M_2 approaches a circular orbit of a fixed radius around M_3 . These simulations were performed for $C_2=0.75$ on a 1000×991 grid with $\Delta x=0.6$, $\Delta t=0.05$, and the terminal time of 5×10^3 (a), 11×10^3 (b), 27×10^3 (c), and 50×10^3 (d) t.u.

structure start “bombarding” vortices of the weaker structure at or near their tips. As it will be shown, this could lead to a breakup of the weaker structure or to its motion as a whole. Reactions between each pair of stable structures of different frequencies are described below. These simulations were done for the base core size, when only S , D , M_2 , and M_3 are stable.

2. M with S

Figure 6(a) shows the vortex tip trajectories during a simulated interaction of M_3^+ with a single vortex S^+ . As it can be seen, M_3 repels S . The outward motion of S occurs along a spiraling trajectory. Similar interaction is observed between M_2 and S , but the coils of the spiraling trajectory of S are more dense and the motion along that trajectory is slower. S^+ and S^- spiral away from any M structure in the clockwise and counterclockwise directions, respectively.

3. M with D

The higher frequency of M_2 or M_3 forces a breakup of D into two separate oppositely charged vortices: $D = S^+ + S^-$. These vortices spiral away from M in opposite directions, as explained above.

4. D with S or D

We observed attraction of S to a simulated periodic point source with the frequency of D . Interaction of S with an actual D is complicated by the inherent motion of the latter. Figure 6(b) shows a simulation, where a simultaneous drift of D and attraction of S lead to their collision. This results in a formation of a stable M_2 , with one S being expelled. This reaction can be represented by a formula

$$D + S^\pm = M_2^\pm + S^\mp. \quad (5)$$

If two D particles collide as a result of their drift towards each other, one M_2 structure is formed and two S vortices are expelled,

$$2D = M_2^\pm + 2S^\mp. \quad (6)$$

The sign of a newly formed M_2 depends on the mutual orientation of dipoles during their collision.

5. M_3 with M_2 (same sign)

M_3 attracts M_2 of the same sign. As shown on Fig. 6(c), M_2 moves towards M_3 along a spiraling trajectory. During their collision a transient five-armed structure is formed that almost immediately breaks up into a stable M_3 and two expelled S vortices. This reaction can be summarized as

$$M_3^+ + M_2^+ = M_3^+ + 2S^+. \quad (7)$$

There is a similar reaction for negative signs. Thus, the long-term effect of M_3 on a like-charged M_2 is a breakup of the latter: $M_2 = 2S$.

6. M_3 with M_2 (opposite signs)

An M_2 structure can rotate around an M_3 structure of the opposite sign, forming a stable “molecule.” The radius of the circular orbit is ≈ 235 d.u. If the initial distance between M_2 and M_3 is different from this radius, the motion of M_2 is described as a limit cycle, with M_2 approaching the circular orbit. Figure 6(d) shows the tip trajectories of M_3^+ and M_2^- in a simulation where the initial distance between these structures is less than the orbit radius. The period of M_2 on the orbit is $\approx 1.86 \times 10^4$ t.u. We also observed stable molecules with several M_2 particles on the same orbit around M_3 .

C. Self-organization

In this section, we explore what happens if a large number of vortices is generated on a large rectangle and the system is allowed to evolve for a long time. Figure 7 summarizes results of two such simulations. Evolution of the initial profile with high vortex density [Fig. 7(a)] is shown on Figs. 7(b) and 7(c) for $C_2=0.75$ and on Fig. 7(d) for $C_2=0.78$.

Figures 7(c) and 7(d) correspond to the simulation time of several thousand rotations of an isolated spiral S and represent the asymptotic behavior of spiral ensembles, i.e., longer simulation times reveal no visible changes in the global pic-

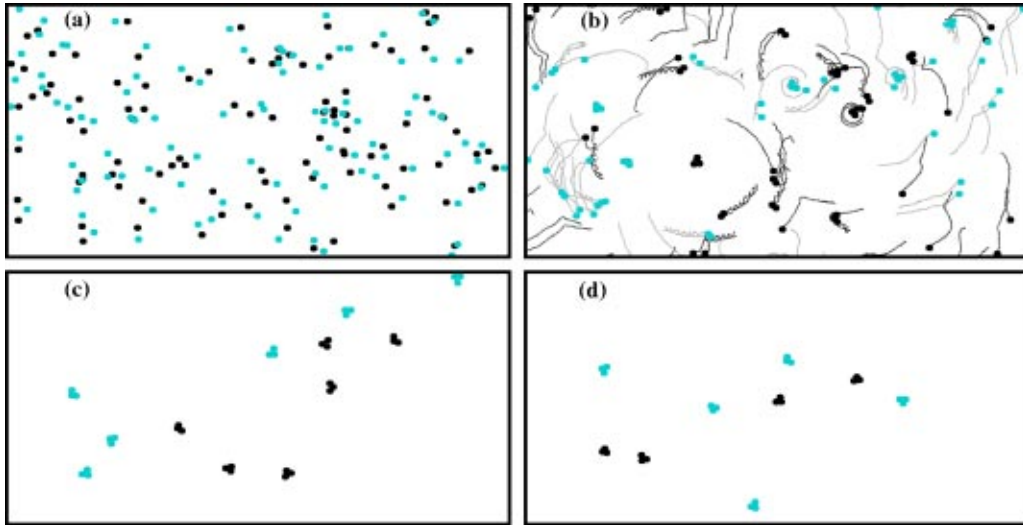


FIG. 7. “Condensation” of spiral gas. Dark and light circles represent, respectively, the positive and negative vortex tips, found by the tip detection algorithm. (a) High initial vortex concentration, created with 100 randomly placed vortex-generating square patches, as explained in Sec. II. The size of the u and v components of each patch was 30×30 d.u. The maximum shift between the components in the x and y directions was 6 d.u. (b) Vortex evolution for the base excitability $C_2 = 0.75$ at $t = 5 \times 10^3$ t.u. The trajectories shown are for $3 \times 10^3 \leq t \leq 5 \times 10^3$. (c) and (d) long-term ($t = 10^5$ t.u.) development for $C_2 = 0.75$ and $C_2 = 0.78$, respectively. These simulations were carried out on a 1498×2989 grid with $\Delta x = 0.6$ and $\Delta t = 0.05$.

ture. As it can be seen in Fig. 7(c), the asymptotic picture for the base value of excitability is dominated by the stable spiral triplets M_3^\pm . Formation, persistence, and eventual domination of such triplets was observed in all experiments with a sufficiently large number of initial vortex-generating patches (over 50). A similar behavior is observed for $C_2 = 0.78$ [Fig. 7(d)], i.e., when the core sizes are approximately twice smaller. For $C_2 = 0.72$, which corresponds to approximately twice larger cores than for the base value, pairs M_2 are the only structures observed in the long term (not shown). Our discussion below will focus on the base value of C_2 , corresponding to Figs. 7(b) and 7(c).

Evolution of the spiral gas occurs according to the reactions described in Sec. III B above. If two initial vortices of the same sign are created within one S wavelength from each other, they attract to form an M_2 pair. If dipoles D are present, an M_2 pair can also appear as a result of a D - S [Fig. 6(b)] or D - D reaction.

There are two mechanisms for M_3 formation. Ensembles M_3 can form at the initial stage from three nearby single vortices of the same sign, which is likely if the initial vortex density is sufficiently high. The second mechanism is not revealed in our list of pairwise reactions. In the presence of multiple high-frequency sources such as M_2 and M_3 , single vortices and M_2 pairs can move along very complex trajectories. Sometimes several like-charge S and M_2 particles collide and form M_3 . These collisions would not occur without a complex surrounding wave pattern. For example, in the absence of other sources, S is repelled from M_2 . Once formed, M_3 particles exhibit amazing stability and almost never disappear. Moreover, they collectively exhibit the strongest influence on the entire medium, breaking up and expelling all other structures.

For low initial vortex densities, whether M_2 or M_3 structures eventually emerge depends on the exact initial profile. The size of the vortex-generating square patches is also important. Patches of smaller size produce dipoles D , which can drift and attract isolated vortices. After the first M_2 or M_3 structures are formed, their waves break up each remaining D into two separate vortices which begin to move in opposite directions.

The total number of vortices in Fig. 7(c) is much lower than in Fig. 7(a). The initial vortex density is lost in two ways: due to recombinations and as a result of collisions with the boundary. Recombinations, i.e., self-annihilation of two colliding vortices of opposite sign, occur very rarely. Most of the initial vortices are “pushed” outside the boundary. Typically, this happens when vortices are repelled by stronger spiral structures. Collisions with the boundary also happen in the case of attraction to remote structures when such attraction occurs along a spiraling trajectory that crosses the boundary.

We observed a similar behavior, including long-term formation and persistence of spiral triplets, in a continuous FHN model with a comparable core size ($\dot{u} = b\Delta u + c[u(d - u)(u - 1) - v]$, $\dot{v} = gu - hv$, with $b = 0.0001$, $c = 0.5$, $d = 0.001$, $g = 0.01$, and $h = 0.04$).

IV. CONCLUSION

In physical excitable media, e.g., in the heart tissue, vortices typically emerge as a result of breaks in the wave fronts, i.e., in the form of dipoles D . Thus, reactions in Eqs. (5) and (6) have a special importance. They explain how higher-order structures can form spontaneously from frequently occurring D and S . The described reactions shed

more light on the possible interactions between multiple wave breaks during the development of some cardiac arrhythmias, such as ventricular fibrillation. In particular, our study suggests a possibility of spontaneously formed stable higher-frequency sources in a fibrillating heart.

A simple model that we used in this study captures only the basic properties of excitable media and can be inadequate in some more complex situations. For example, in the case of BZ reaction reported by Agladze and Krinsky [6], the frequency of multiarmed spirals decreased with increasing number of arms. However, our investigation elucidates important interaction patterns of a large number of vortices and sets a framework for similar studies for each specific medium.

The presented results reveal three levels of possible self-organization in active media. Existence of persistent excitation vortices and simple spirals can be viewed as the first level. Formation of stable vortex ensembles constitutes the second level. The third level of self-organization, which to our knowledge has never been reported before, is the ability of ensembles to interact with each other and form superstructures, such as the described M_3 - M_2 molecule, or organize into global patterns, such as the coexisting triplets. Thus, an excitable medium can exhibit emergent [21] behavior, i.e., relatively simple rules that describe its local properties lead to unexpected complex global properties, not apparent from the local rules.

The spiral gas evolves into a “triplet gas” in a broad range of parameters. However, to observe such an evolution,

the medium has to be sufficiently large to accommodate a large number of interacting spirals, and the experiment duration has to be sufficiently long, such as several thousand isolated spiral periods, which corresponds to numerical simulations of demanding computational intensity. Moreover, the emergence of triplets is observed only if the initial vortex concentration is sufficiently high, with the distance between neighboring vortices comparable to one isolated spiral wavelength.

To reduce the loss of vortex density in a spiral gas, topologies without boundaries, such as sphere or torus, can be considered. In these topologies the total charge is conserved and a high initial vortex concentration can decrease only due to recombinations. This may result in a richer and more interesting spectrum of particle interactions.

A laser beam can be used to generate, control, and annihilate excitation vortices in some BZ media [9]. A laser and a charge-coupled device can also be used to “read” an excitation pattern. Thus, vortices in such media can be used to store information. Further research of stable spiral structures may lead to ideas on how to use their interaction patterns as a basis of *computing* process.

ACKNOWLEDGMENT

This research was supported in part by the National Heart, Lung, and Blood Institute of the National Institutes of Health, Grant No. 2PO1-HL-39707.

-
- [1] A.N. Zaikin and A.M. Zhabotinsky, *Nature (London)* **255**, 535 (1970); A.T. Winfree, *Science* **175**, 634 (1972).
 - [2] J.M. Davidenko, A.M. Pertsov, R. Salomonsz, W. Baxter, and J. Jalife, *Nature (London)* **355**, 349 (1992).
 - [3] K.J. Lee, E.C. Cox, and R.E. Goldstein, *Phys. Rev. Lett.* **76**, 1174 (1996).
 - [4] M. Bär, I.G. Kevrekidis, H.-H. Rotermund, and G. Ertl, *Phys. Rev. E* **52**, 5739 (1995).
 - [5] F.X. Witkowski, L.J. Leon, P.A. Penkoske, W.R. Giles, M.L. Spano, W.L. Ditto, and A.T. Winfree, *Nature (London)* **392**, 78 (1998).
 - [6] K.I. Agladze and V.I. Krinsky, *Nature (London)* **296**, 424 (1982).
 - [7] V.I. Krinsky and K.I. Agladze, *Physica D* **8**, 50 (1983).
 - [8] E.A. Ermakova, A.M. Pertsov, and E.E. Shnol, *Physica D* **40**, 185 (1989).
 - [9] O. Steinbock and S.C. Müller, *Int. J. Bifurcation Chaos Appl. Sci. Eng.* **3**, 437 (1993).
 - [10] M. Ruiz-Villarreal, M. Gómez-Gesteira, C. Souto, A.P. Muñozuri, and V. Pérez-Villar, *Phys. Rev. E* **54**, 2999 (1996).
 - [11] I. Aranson, H. Levine, and L. Tsimring, *Phys. Rev. Lett.* **76**, 1170 (1996).
 - [12] B. Vasiev, F. Siegert, and C. Weijer, *Phys. Rev. Lett.* **78**, 2489 (1997).
 - [13] I. Schebesch and H. Engel, *Phys. Rev. E* **60**, 6429 (1999).
 - [14] I.S. Aranson and L.M. Pismen, *Phys. Rev. Lett.* **84**, 634 (2000).
 - [15] I.S. Aranson, L. Kramer, and A. Weber, *Phys. Rev. Lett.* **67**, 404 (1991).
 - [16] X.-J. Li, H.-W. Xi, and J.D. Gunton, *Phys. Rev. E* **54**, R3105 (1996).
 - [17] R. FitzHugh, *Biophys. J.* **1**, 445 (1961); I. Nagumo, S. Yoshizawa, and S. Arimoto, *IEEE Trans. Commun. Technol.* **12**, 400 (1965).
 - [18] Y.A. Ermakova, V.I. Krinskii, A.V. Panfilov, and A.M. Pertsov, *Biophysics (Engl. Transl.)* **31**, 348 (1986).
 - [19] G. Gottwald, A. Pumir, and V. Krinsky, *Chaos* **11**, 487 (2001).
 - [20] R.M. Zaritski and A.M. Pertsov, in *Proceedings of Neural, Parallel, and Scientific Computations*, edited by M.P. Bekakos, G.S. Ladde, N.G. Medhin, and M. Sambandham (Dynamic Publishers, Atlanta, 2002), Vol. 2, p. 187.
 - [21] J.H. Holland, *Emergence: From Chaos to Order* (Addison-Wesley, Reading, MA, 1998).